Cell Reports

Report

Organization of Mitochondrial Gene Expression in Two Distinct Ribosome-Containing Assemblies

Graphical Abstract

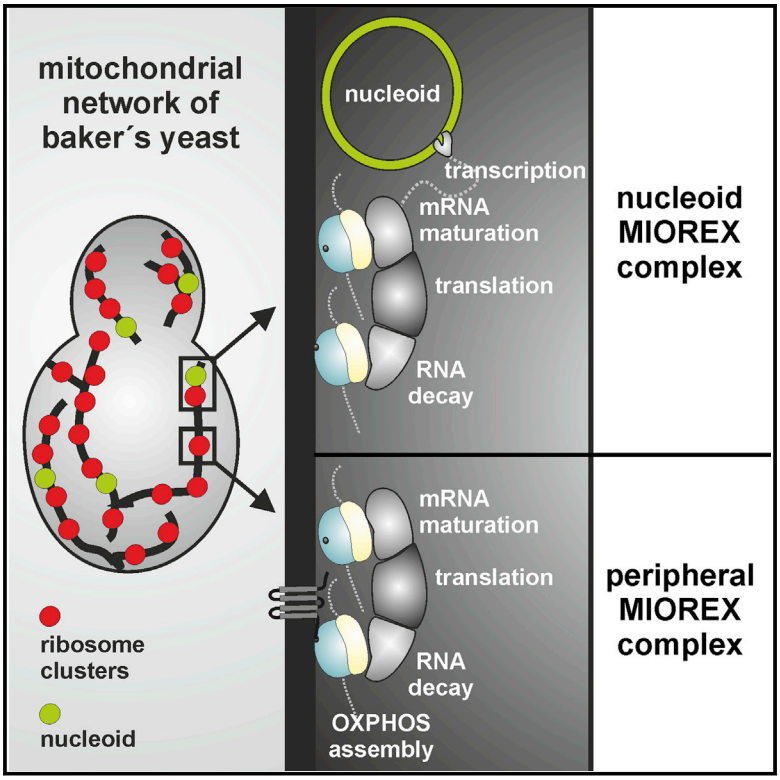

Highlights

- Mitochondrial ribosomes have a large interactome, resulting in MIOREX complexes
- MIOREX complexes organize ribosomes and mRNA metabolism in large assemblies
- A subset of the MIOREX complexes is associated with the nucleoid
- MIOREX complexes channel gene expression from transcription to translation

Authors

Kirsten Kehrein, Ramon Schilling, ..., Thomas Langer, Martin Ott

Correspondence

martin.ott@dbb.su.se

In Brief

Mitochondria have a complete genetic system necessary for the biogenesis of the respiratory chain. Kehrein et al. utilize biochemical fractionation and superresolution microscopy to identify large clusters of mitochondrial ribosomes interacting with proteins implicated in posttranscriptional mRNA metabolism and respiratory chain assembly to create expressosome-like assemblies, the MIOREX complexes.

Kehrein et al., 2015, Cell Reports *10*, 843–853
February 17, 2015
http://dx.doi.org/10.1016/j.celrep.2015.01.012

CellPress

Cell Reports
Report

Organization of Mitochondrial Gene Expression in Two Distinct Ribosome-Containing Assemblies

Kirsten Kehrein,[1] Ramon Schilling,[1] Braulio Vargas Möller-Hergt,[1] Christian A. Wurm,[2] Stefan Jakobs,[2,3,4] Tobias Lamkemeyer,[5] Thomas Langer,[5,6,7,8] and Martin Ott[1,*]
[1]Center for Biomembrane Research, Department of Biochemistry and Biophysics, Stockholm University, 106 91 Stockholm, Sweden
[2]Department of NanoBiophotonics, Max Planck Institute for Biophysical Chemistry, 37070 Göttingen, Germany
[3]Department of Neurology, University of Göttingen Medical School, 37073 Göttingen, Germany
[4]Center Nanoscale Microscopy and Molecular Physiology of the Brain (CNMPB), 37073 Göttingen, Germany
[5]Cologne Excellence Cluster on Cellular Stress Responses in Aging-Associated Diseases (CECAD), University of Cologne, 50931 Cologne, Germany
[6]Institute for Genetics, University of Cologne, 50931 Cologne, Germany
[7]Center for Molecular Medicine (CMMC), University of Cologne, 50931 Cologne, Germany
[8]Max-Planck-Institute for Biology of Aging, 50931 Cologne, Germany
*Correspondence: martin.ott@dbb.su.se
http://dx.doi.org/10.1016/j.celrep.2015.01.012

SUMMARY

Mitochondria contain their own genetic system that provides subunits of the complexes driving oxidative phosphorylation. A quarter of the mitochondrial proteome participates in gene expression, but how all these factors are orchestrated and spatially organized is currently unknown. Here, we established a method to purify and analyze native and intact complexes of mitochondrial ribosomes. Quantitative mass spectrometry revealed extensive interactions of ribosomes with factors involved in all the steps of posttranscriptional gene expression. These interactions result in large expressosome-like assemblies that we termed mitochondrial organization of gene expression (MIOREX) complexes. Superresolution microscopy revealed that most MIOREX complexes are evenly distributed throughout the mitochondrial network, whereas a subset is present as nucleoid-MIOREX complexes that unite the whole spectrum of organellar gene expression. Our work therefore provides a conceptual framework for the spatial organization of mitochondrial protein synthesis that likely developed to facilitate gene expression in the organelle.

INTRODUCTION

Mitochondrial gene expression provides a small set of essential subunits to the oxidative phosphorylation system (OXPHOS) (Hällberg and Larsson, 2014). Proteins involved in expression and assembly of the mitochondrially encoded translation products represent a quarter of the mitochondrial proteome of baker's yeast (Sickmann et al., 2003), and this genetic system contains complete machineries for DNA replication, repair, and transcription; for RNA modification, mRNA maturation/splicing, and RNA degradation; and for protein synthesis. How these proteins cooperate to mediate efficient protein synthesis and how they are organized in time and space is currently not known.

Mitochondrial ribosomes developed from those of the bacterial ancestor of the organelle and were significantly remodeled during evolution; they contain many mitochondria-specific protein subunits and have a reduced rRNA content (Kehrein et al., 2013; Smits et al., 2007). This modified composition was accompanied by the development of mitochondria-specific features of translation. Prime examples for this are specific translational activators that are required for translation of a single species of mRNA (Costanzo and Fox, 1990; Fox, 2012). Recent work has demonstrated that translational activators coordinate mitochondrial and nuclear gene expression to facilitate biogenesis of the OXPHOS (Gruschke et al., 2012; Mick et al., 2011). In the case of cytochrome *b* biogenesis, this feedback loop involves binding of a translational activator complex to the ribosomal tunnel exit to enable efficient interaction of the newly synthesized protein with an assembly factor (Gruschke et al., 2011).

Because of this rather unique organization of protein synthesis in mitochondria, we asked how mitochondrial ribosomes are generally organized and whether factors involved in the biogenesis of the other mitochondrially encoded proteins also interact with the mitochondrial ribosome. We established a method to purify and analyze native and intact mitochondrial ribosome complexes. Mass spectrometric analyses revealed extensive interactions of this translation machinery with factors involved in various posttranscriptional steps of gene expression. Likewise, we identified many proteins without annotated function. Employing biochemical fractionations and superresolution microscopy, we show that mitochondrial ribosomes are forming distinct clusters that we term mitochondrial organization of gene expression (MIOREX) complexes. A subset of these clusters is engaged in a large complex with the nucleoid that unites transcription, mRNA maturation, translation, and RNA decay. The organization

of ribosomes in the MIOREX complexes likely allows channeling of the transcripts from maturation to translation and decay and demonstrates that mitochondrial gene expression is much higher organized than previously known.

RESULTS

Mitochondrial Ribosomes Have a Large Interactome

In order to identify the proteome and interactome of the mitochondrial ribosome, we set out to establish conditions by which intact ribosomes can be analyzed biochemically. Isolated yeast mitochondria were purified by step-gradient centrifugation, and detergent lysates of these preparations were separated on linear sucrose gradients. Magnesium is important to stabilize the folds of RNAs and, consequently, their interactions with proteins. Unexpectedly, the ribosomal subunits smeared instead of forming clear peaks in the presence of magnesium (Figure 1A). Because degradation products of the ribosomal proteins were not detected, this migration behavior could reflect a degradation of the rRNAs and hence disintegration of the ribosomes. We tested this by adding EDTA to the lysis buffer to inhibit RNases (Figure 1B). Under these conditions, the small and large subunits formed clear peaks and no free ribosomal proteins were detected in the load. However, whereas EDTA is an excellent RNase inhibitor, chelating magnesium dissociates mitochondrial ribosomes and their interacting factors as seen before for cytoplasmic ribosomes.

We tested other RNase inhibitors, but they did not inhibit the disintegration of ribosomes in lysates prepared with magnesium. We therefore genetically removed the main unspecific mitochondrial nuclease Nuc1 (Vincent et al., 1988) and analyzed by northern blotting its effect on the stability of rRNAs. When incubated for 15 min on ice, the 21S and the 15S rRNAs were substantially degraded in lysates of wild-type mitochondria (Figure 1C), likely accounting for the observed smearing of ribosomal subunits in the gradients (Figure 1A). Importantly, absence of Nuc1 clearly stabilized the rRNAs as well as the tRNAs (Figure 1C). We next optimized the conditions for ribosome fractionation further by increasing the magnesium concentration and adding spermidine to stabilize ribosomal interactions. Employing these conditions, the ribosomes were almost exclusively found in the bottom fraction, indicating that they are part of a large complex (Figure 1D). Next, we analyzed ribosome complexes at different ionic strength on sucrose gradients. Quantification of the relative signals of the large subunit demonstrated that the ribosomes migrated as increasingly smaller particles with increasing ionic strength (Figures 1E and 1F). This indicated that mitochondrial ribosomes have a large interactome that dissolves in a salt-dependent fashion.

Ribosome Complexes Contain Many Factors Involved in Mitochondrial Gene Expression

We next aimed at identifying this large, previously uncharacterized interactome of the mitochondrial ribosome. Mitochondrial ribosomes and their interaction partners were immunoprecipitated under mild conditions, and the complexes were analyzed by label-free, quantitative mass spectrometry (Figures 2A and 2B). It was exciting to see that many factors known to participate in mitochondrial gene expression were specifically enriched when ribosomes were purified at 10 mM KOAc (Figures 2C and 2E; Table S1). As expected by previous results demonstrating genetic interactions of translational activators with the mitochondrial ribosome (Haffter et al., 1990, 1991), most of the translational activators were recovered with the mitochondrial ribosome. Unexpectedly, we also found many proteins involved in mRNA maturation and processing, DNA metabolism and organization of the nucleoid, and some factors implicated in OXPHOS assembly together with previously uncharacterized proteins that we termed Mrx1–Mrx13 proteins (Figure 2E; Table S1).

To sort this complex interactome into loose and tight interactors, we purified mitochondrial ribosomes under rather harsh ionic strength conditions (300 mM KOAc), where most of the interactors are lost (Figures 1D and 1E). Mass spectrometry identified all subunits of the small and the large ribosomal subunit (Figure 2D), with three exceptions that do not behave as ribosomal proteins (Mrps2, Mrp8 [Figure S1], and Ymr31/Kgd4; Heublein et al., 2014). This showed that ribosomes containing intact small and large subunits could be purified under these conditions, thus revealing the exact composition of the ribosome.

A number of additional proteins were copurified at 300 mM KOAc (Figure 2E, protein names in bold): proteins involved in RNA metabolism and previously uncharacterized proteins including Ydr115p and Ynl122p, homologs of the bacterial ribosomal proteins L34 and L35, respectively (Figure 2E; Table S2). It was somewhat unexpected to find that even four translational activators interact rather firmly with the ribosome (Figure 2E). Taken together, our analyses of native ribosome complexes suggested that mitochondrial ribosomes interact with factors involved in general gene expression. Importantly, this large, complex interactome was in line with our previous biochemical fractionations (Figure 1) and pointed to a previously unrecognized organization of mitochondrial gene expression.

Proteins Involved in Mitochondrial Gene Expression Interact with Mitochondrial Ribosomes

In order to determine how quantitative these interactions are, we analyzed comigration of selected representatives of each class of interactors with the ribosome. To discriminate between tight and lose binders, we employed conditions of low (10 mM KOAc) and intermediate (100 mM KOAc) ionic strength, respectively. As observed before (Figure 1F), increasing the ionic strength shifted the ribosome from the bottom fraction to the middle of the gradient (Figure 3B).

The major molecular chaperones (Hsp70 and Hsp60) and other soluble proteins (Aco1) did not comigrate with the ribosome (Figures 3A and 3B). The previously studied ribosome-membrane-anchoring proteins Mdm38 and Oxa1 (Frazier et al., 2006; Jia et al., 2003; Szyrach et al., 2003) interacted only to a minor extent with the ribosomes at low salt and were released at higher salt concentrations (Figures 3A and 3B), whereas the ribosome receptor Mba1 did not comigrate with ribosomes under these conditions. However, the interaction of Mba1 with the ribosome has been detected even by chemical crosslinking in intact organelles (Gruschke et al., 2010). This observation therefore suggests that the conditions established here are still

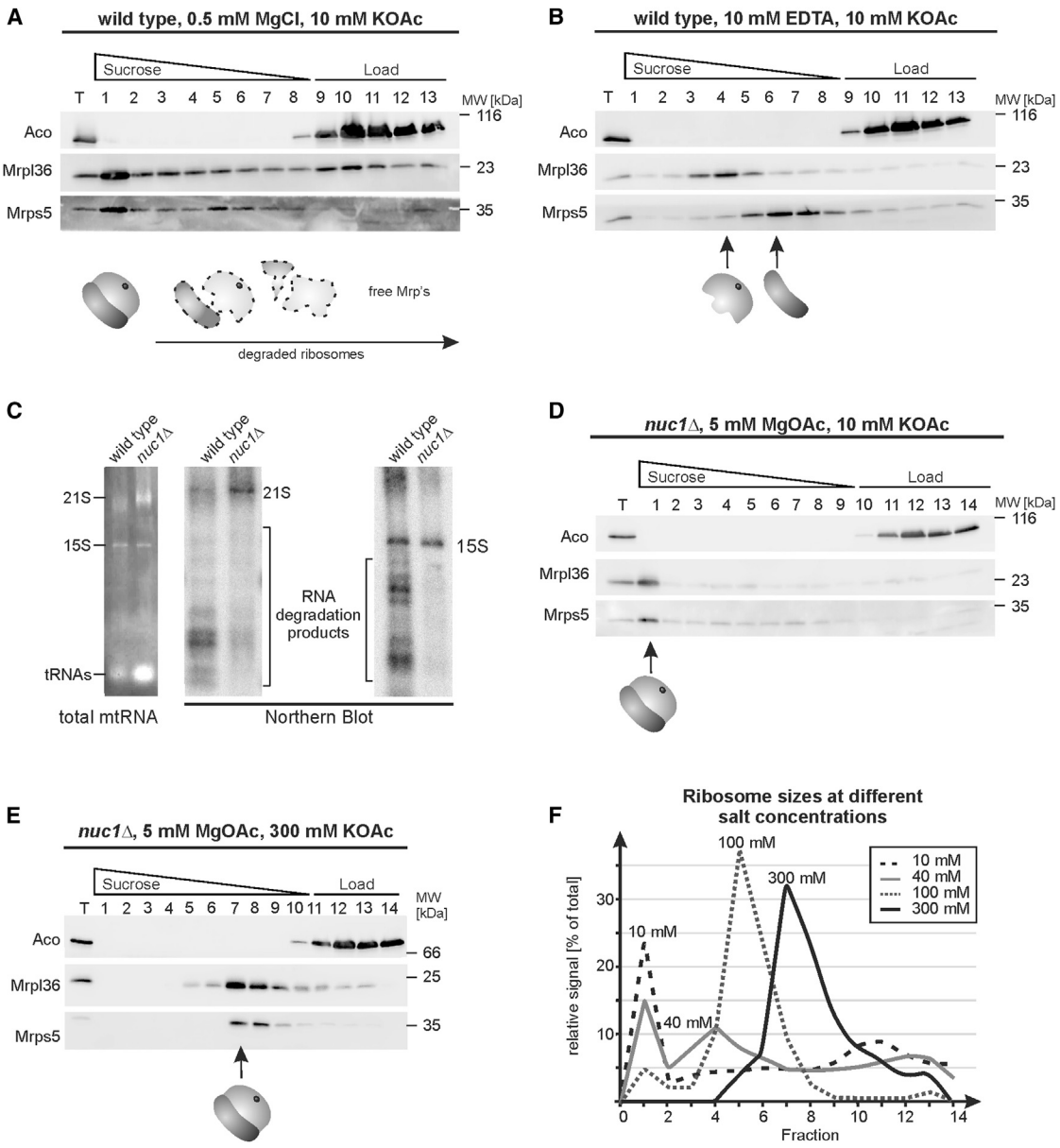

Figure 1. Mitochondrial Ribosomes Have a Large Interactome

(A) Isolated mitochondria were lysed for 30 min and subjected to velocity centrifugation on a linear sucrose gradient. Fractions were analyzed by western blotting. MW, molecular weight; T, total (representing 10% of the starting material).

(B) Isolated mitochondria were lysed in a buffer containing 10 mM EDTA and analyzed as described in Figure 1A.

(C) Isolated mitochondria from the indicated strains were lysed and incubated as in (A). RNA was extracted and analyzed by northern blotting.

(D and E) Isolated mitochondria were lysed for 10 min on ice and subjected to velocity centrifugation on a linear sucrose gradient.

(F) The signal of Mrpl36 in sucrose gradients was analyzed densiometrically from lysates prepared with 10 mM, 40 mM, 100 mM, and 300 mM KOAc, respectively.

not gentle enough to maintain ribosome interactions of this and possibly other similarly weak binding proteins.

The translational activator complex Cbp3-Cbp6 is present at steady state mostly in a nonribosome-bound assembly intermediate (Gruschke et al., 2012), explaining why only a fraction of the complex comigrated with the ribosome (Figures 3A and 3B). In contrast, Mss51 that plays a similar role in the biogenesis of Cox1 (Mick et al., 2011) did not interact with the ribosome (Figures 3A and 3B; Table S1). Interestingly, the Atp9-specific biogenesis factor and translational activator Atp25 (Zeng et al., 2008) comigrated quantitatively with the large ribosomal subunit even at intermediate ionic strength, revealing a surprisingly tight binding (Figures 2E, 3A, and 3B).

Strong enrichment in the ribosomal fraction was also observed for the RNA helicase Mrh4 or the guanosine triphosphatase (GTPase) Mtg2 that play different roles in ribosome assembly

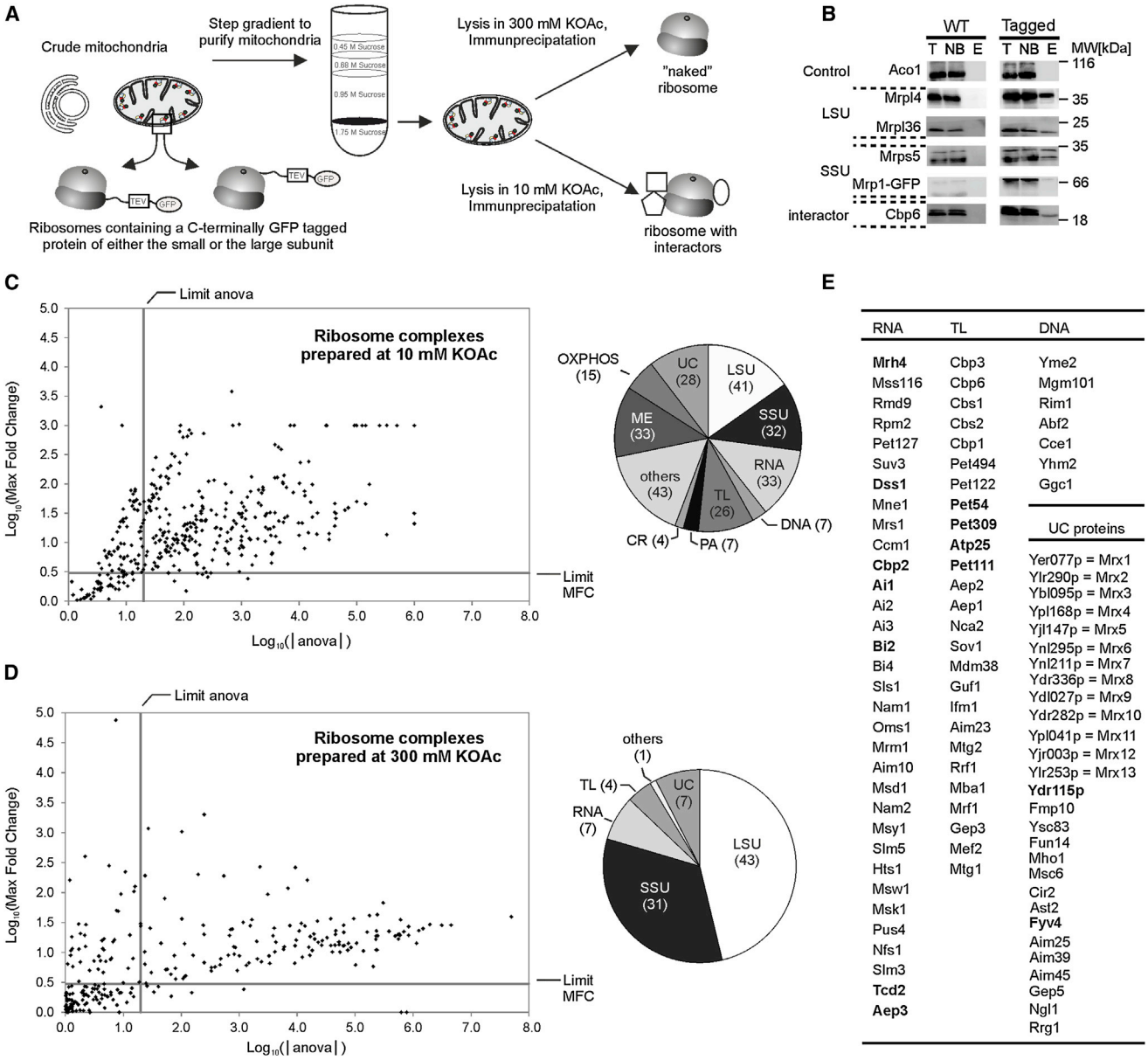

Figure 2. Ribosome Complexes Contain Many Factors Involved in Mitochondrial Gene Expression

(A) Schematic of the experimental procedure for the purification of the mitochondrial ribosome and its interactors.

(B) Ribosomes were purified with Mrp1-GFP, and the purification was compared to an untagged control. E, eluate; LSU, large ribosomal subunit; NB, not bound; SSU, small ribosomal subunit; T, starting material; WT, wild-type.

(C) Mitochondria from a strain with Mrp1-GFP were lysed and ribosomes purified under low-salt conditions (10 mM KOAc). All proteins identified in the eluates that were enriched at least three times over background (max fold change $\leq$ 3) and with a significance value (ANOVA) of $\leq$0.05 were considered in the analysis. Numbers in brackets indicate the sum of proteins identified for the different protein classes. CR, chaperones; DNA, proteins involved in DNA metabolism; ME, metabolic enzymes; OXPHOS, components of the oxidative phosphorylation system; PA, proteases; RNA, proteins involved in RNA metabolism; TL, translation; UC, uncharacterized proteins;

(D) Mitochondria from a strain encoding a chromosomally GFP-tagged variant of Mrpl4 were lysed and ribosomes purified under high-salt conditions (300 mM KOAc). Numbers in brackets indicate the sum of proteins identified for the different protein classes.

(E) Copurified proteins implicated in RNA and DNA metabolism and translation and uncharacterized proteins are shown; bold letters indicate that the proteins were also found in ribosomes prepared under high ionic strength.

See also Tables S1 and S2.

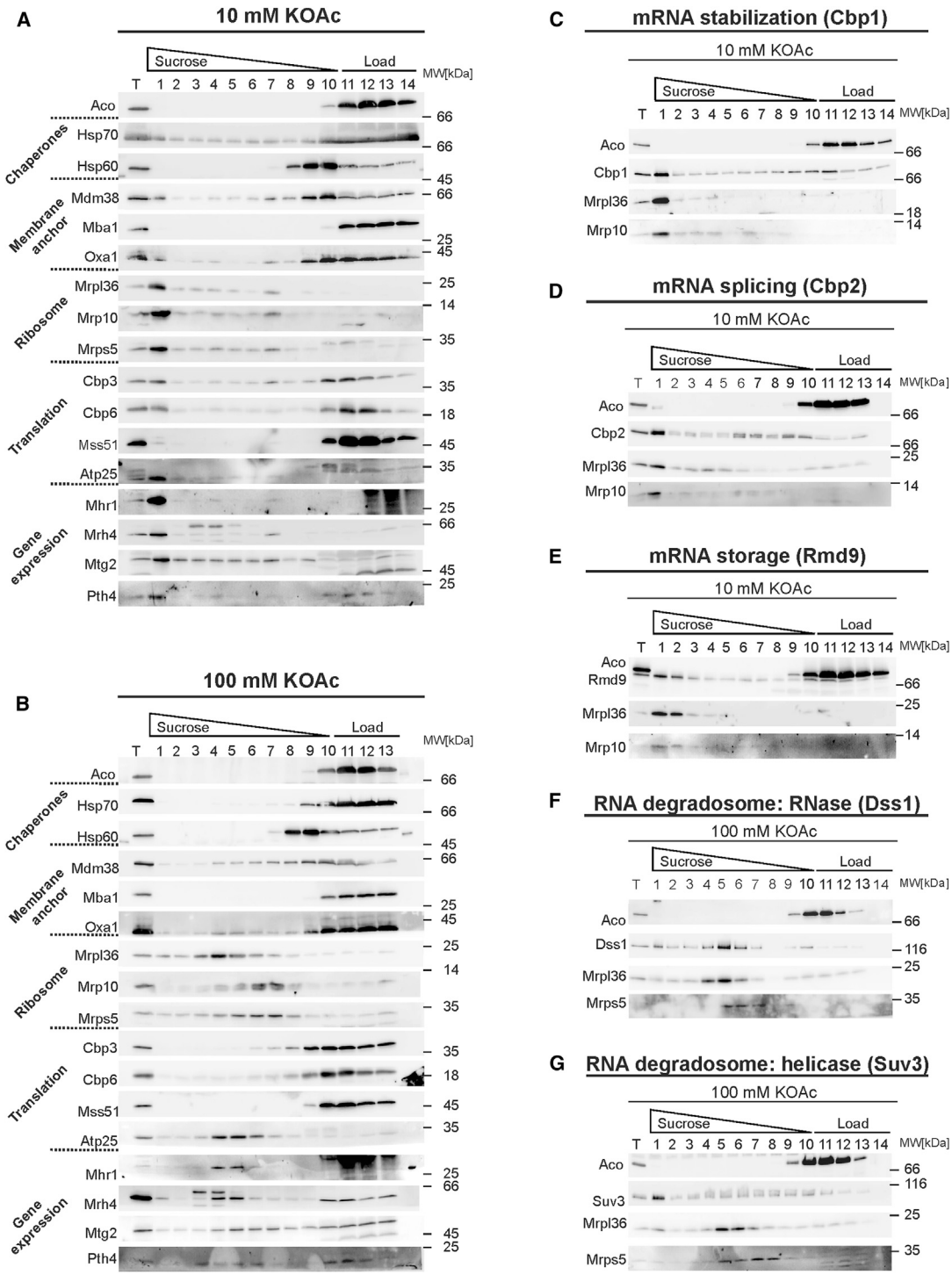

Figure 3. Proteins Involved in Mitochondrial Gene Expression Interact with Ribosomes in the MIOREX Complexes

(A) Mitochondria were lysed in a buffer with 10 mM KOAc and processed as in Figure 1D. Proteins were analyzed by western blotting using the indicated antibodies.

(B) Mitochondria were lysed in a buffer with 100 mM KOAc and processed as in Figure 1D. Proteins were analyzed by western blotting using the indicated antibodies.

(C–G) Mitochondria were lysed and processed as in (A) or (B). Proteins were analyzed by western blotting using the indicated antibodies. T, 10% total before centrifugation on sucrose gradients.

See also Figure S2.

(Datta et al., 2005; De Silva et al., 2013; Figures 3A and 3B). Mhr1, which is implicated in homologous recombination of mitochondrial DNA (Ling and Shibata, 2002), comigrated with the large subunit, in line with structural data (Amunts et al., 2014). In contrast, the ICT1 homolog Pth4 (Figure 3A) was present in a ribosome-bound and in a free form, supporting the idea of a dual role as a ribosomal subunit and as a peptidyl-tRNA hydrolase (Greber et al., 2014; Richter et al., 2010). Taken together, all tested proteins that were specifically copurified with the ribosome (Figure 2) interacted to a substantial extent with the ribosome in these detailed analyses.

Factors of Posttranscriptional RNA Metabolism Bind to the Ribosome

To test for comigration of proteins involved in mRNA metabolism, we constructed tagged variants of representative proteins and followed their migration under low and intermediate salt conditions (Figures 3C–3G and S2). As seen before for the translational activators Atp25 and Cbp3-Cbp6 (Figure 3A), proteins implicated in stabilization of mRNAs (Cbp1), splicing (Cbp2), mRNA storage (Rmd9), or components of the RNA degradosome (Dss1 and Suv3) comigrated with mitochondrial ribosomes under low ionic strength conditions, thereby confirming the copurification results Figures 2E and S2. Dss1 (Figure 3F), the nuclease subunit of the RNA degradosome, was mainly comigrating with the large ribosomal subunit also at increased ionic strength. Interestingly, the helicase Suv3, the other subunit of the RNA degradosome (Figure 3G) was clearly part of a very large complex.

In summary, our analyses revealed that proteins implicated in mitochondrial gene expression interact specifically with mitochondrial ribosomes. Because these interactions result in highly complex assemblies that represent a novel way to organize gene expression, we named them MIOREX complexes to highlight that these complexes are conceptually very different from ribosomes exclusively involved in translation.

MIOREX Complexes Form Distinct Clusters

The most surprising ribosome interactors revealed from our mass spectrometric analyses were components involved in DNA metabolism. This suggested that MIOREX complexes and the nucleoid could be engaged in an additional assembly, giving rise to distinct MIOREX complexes. To detect such very large nucleoid-MIOREX complexes, we decreased the centrifugation speed and time and repeated our analyses of lysates prepared under low ionic strength conditions. A large complex was found at the bottom of the gradient also under these conditions that contained the nucleoid markers Abf2 and Mgm101 (Figure 4A) and a fraction of the ribosomes together with translational activators (Cbp3-Cbp6 and Atp25) and factors involved in ribosome assembly (Mtg2), RNA helicases (Mrh4), and RNA decay (Suv3). This nucleoid-MIOREX complex therefore represents an additional assembly that unites the whole genetic system.

Importantly, MIOREX complexes did not quantitatively associate with the nucleoid, because most ribosomes sediment under these conditions as substantially smaller complexes of a nonetheless specific size (Figure 4A). Interestingly, the translational activators Cbp3-Cbp6 and Atp25, the RNA helicase Mrh4, and the GTPase Mtg2 comigrated with the ribosomes also in these smaller complexes (Figure 4A). The translational activator Cbs2 was present in the nucleoid-MIOREX complex (Figure 4B, fraction 1) in nucleoid-free MIOREX complexes (fractions 9–13) and in ribosome-free complexes of larger size (fractions 5–8) of unknown composition. Importantly, even factors involved in splicing (Cbp2) or stabilization of *COB* mRNA (Cbp1) or in general mRNA storage (Rmd9) fractionated with both MIOREX complexes and were not enriched in the fraction containing the nucleoid-MIOREX complex (Figures 4C–4E), confirming that protein synthesis and mRNA metabolism are tightly linked in these smaller MIOREX complexes that are not interacting with the nucleoid.

Taken together, these results demonstrated that MIOREX complexes are found in two fundamentally different assemblies, namely those engaging the nucleoid and those without nucleoid interactions, and that all MIOREX complexes are equipped with factors involved in mRNA metabolism like splicing, storage, or RNA decay.

Distribution of MIOREX Cluster in Mitochondria

The finding that ribosomes are present in two different MIOREX complexes prompted us to determine how ribosomes are localized in the mitochondrial network. To this end, we employed stimulated emission depletion (STED) superresolution microscopy in combination with immunofluorescence labeling (Jakobs and Wurm, 2014). To determine the submitochondrial localization of MIOREX complexes, we chromosomally GFP-tagged proteins and used antibodies directed against GFP to detect their localization (Figure 5A). This approach revealed that mitochondrial ribosomes as exemplified by Mrpl4-GFP (that is part of both MIOREX complexes; Figure S3) are localized in clusters that are evenly distributed throughout the mitochondrial tubules (Figure 5A). We found a subset of ribosome clusters adjacent to (Figure 5A, *) or colocalizing (Figure 5A, **) with mtDNA, which presumably reflects the nucleoid-MIOREX complexes. Consistently, the RNA storage factor Rmd9 (Nouet et al., 2007; Williams et al., 2007), a component of the MIOREX complexes (Figure 3E), was found in distinct clusters that were similarly distributed in the mitochondrial tubules (Figures 5A and 5B). In contrast, ATP-synthase, as evidenced by immunostaining against Atp4-GFP, had a uniform distribution and was not found in distinct clusters (Figure 5C). In summary, the distributions of mitochondrial ribosomes and nucleoids, as revealed by superresolution microscopy, are in agreement with our biochemical data that demonstrate the existence of two different ribosome-containing clusters, namely the nucleoid-MIOREX assembly and the peripheral MIOREX clusters.

DISCUSSION

In recent years, novel approaches and methodological innovations have changed our view on the organization of general functions in mitochondria. The emerging picture is that many processes are organized in higher-ordered assemblies as exemplified by the respiratory chain supercomplexes (Schägger and Pfeiffer, 2000), ER-mitochondria encounter structure complexes involved in organellar biogenesis and inheritance (Kornmann and Walter, 2010), mitochondrial contact site and cristae organizing

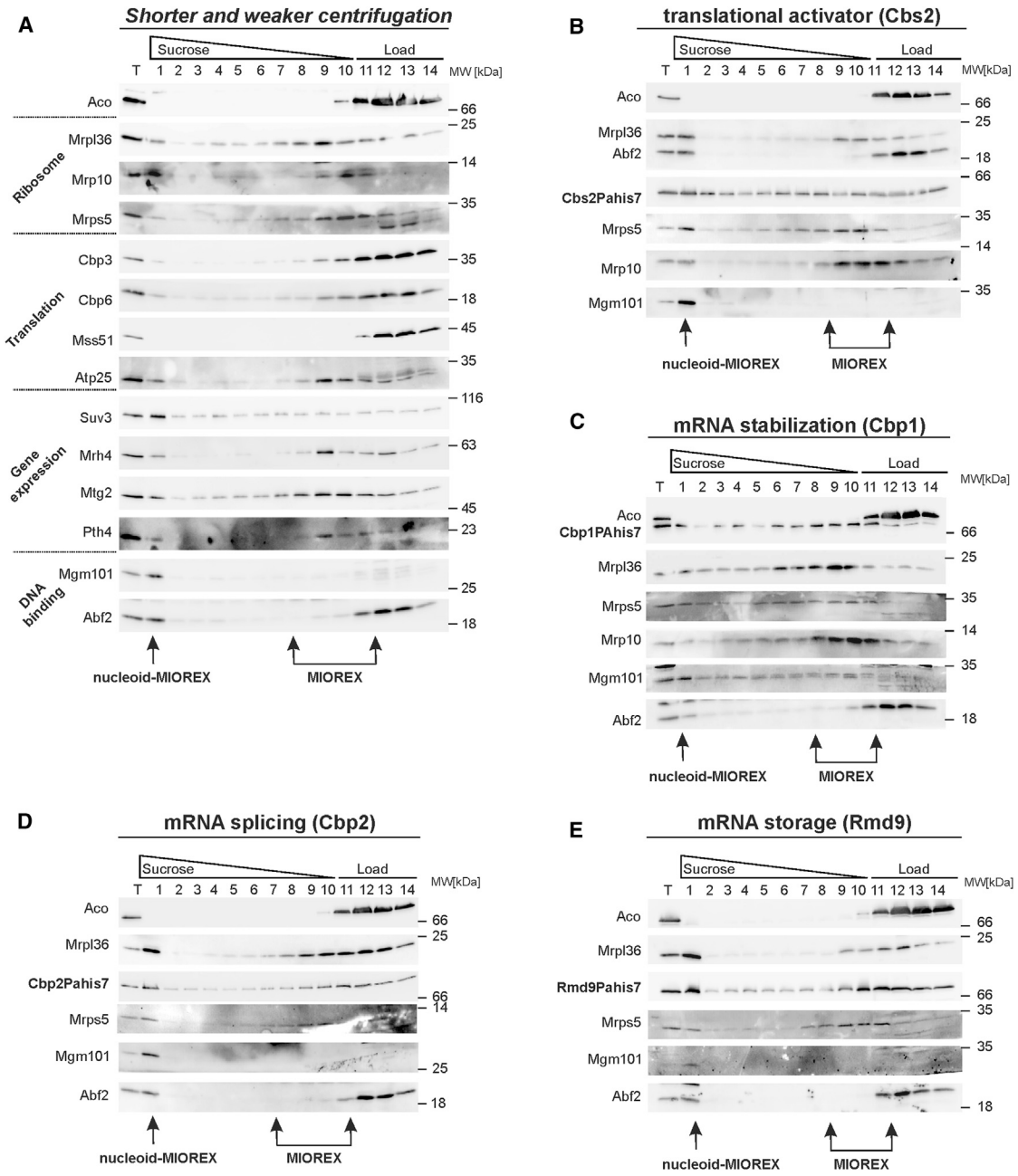

Figure 4. MIOREX Complexes Exist in Nucleoid-Associated and Nonnucleoid-Associated Forms

(A) Mitochondria containing a chromosomally PAhis7-tagged variant of Suv3 were lysed as described in Figure 1D and separated on a sucrose gradient for 30 min at 185,000 × *g*.

(B–E) Migration behavior of PAhis7-tagged variants of proteins involved in *COB* mRNA expression under reduced centrifugation conditions as in (A).

system complexes responsible for the organization of mitochondrial ultrastructure and biogenesis (Harner et al., 2011; Hoppins et al., 2011; von der Malsburg et al., 2011), and translocase of the inner mitochondrial membrane-translocase of the outer mitochondrial membrane supercomplexes mediating protein import (Chacinska et al., 2003). Here, we identified a similar higher-order organization of mitochondrial ribosomes that form large assemblies containing multiple factors involved in gene expression that we termed MIOREX complexes. These complexes are either found in close proximity to the mitochondrial nucleoid (nucleoid-MIOREX complexes) or distributed along the mitochondrial reticulum to form peripheral MIOREX complexes.

Data presented in this manuscript suggest that MIOREX complexes organize mitochondrial gene expression by coupling posttranscriptional mRNA metabolism and translation of the mRNAs with mRNA decay (Figure 5D). Several recent studies

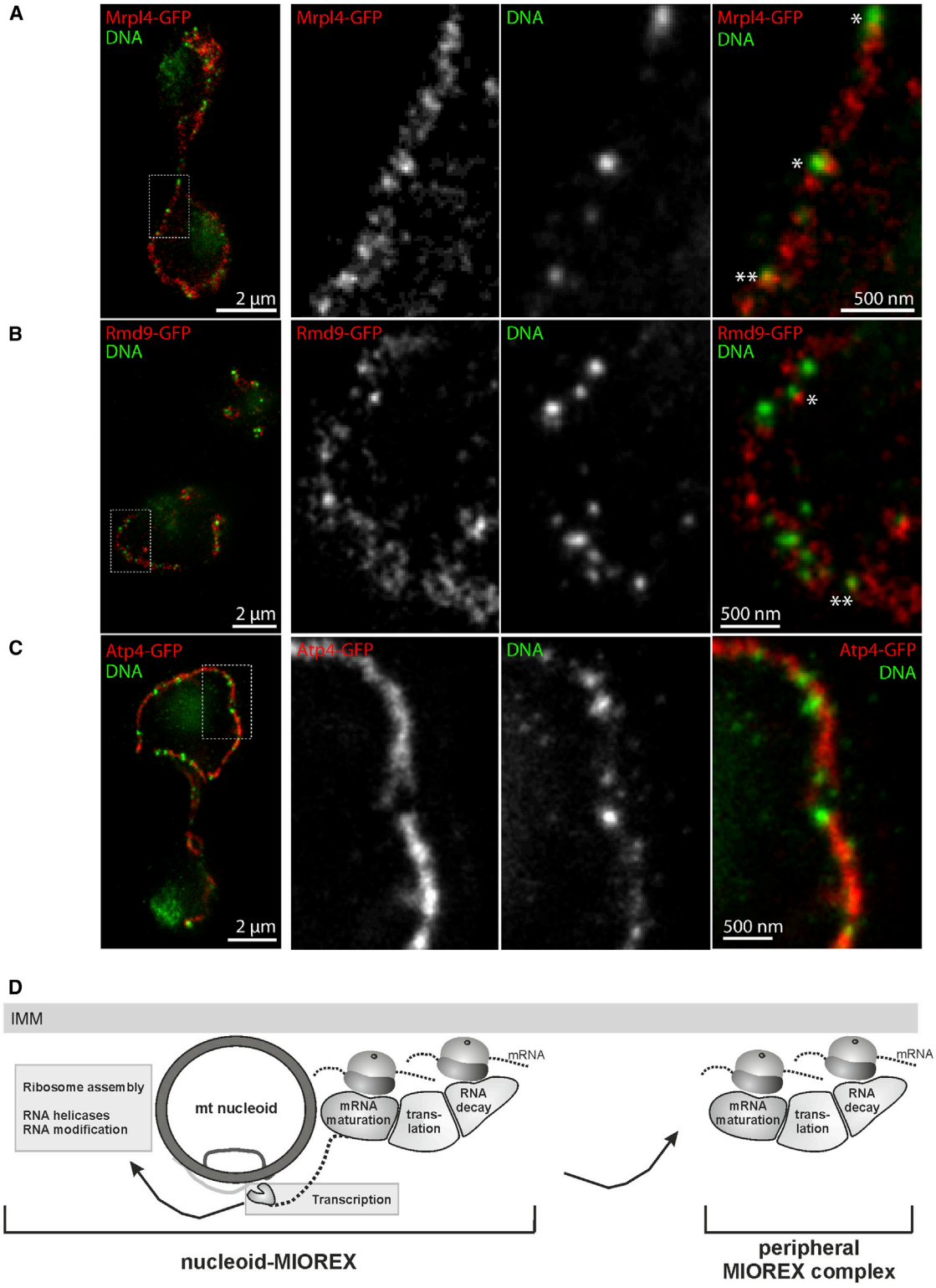

Figure 5. Distribution of MIOREX Complexes in the Mitochondrial Network

(A–C) Dual-color STED superresolution microscopy of the mitochondrial nucleoids (DNA) together with the mitochondrial ribosomes (A, Mrpl4-GFP), the mRNA storage protein Rmd9 (B, Rmd9-GFP), or a subunit of the F_1F_O-ATPase (C, Atp4-GFP). Left to right: dual-color overview image; nucleoids are shown in green. Magnifications of the boxed areas show the localizations of the indicated proteins. Overlay of the magnified areas. The optical resolution in these images was

(legend continued on next page)

in mammalian cells have shown that RNA degradation and newly transcribed RNA are found in foci that are located in vicinity to the mitochondrial DNA (Antonicka et al., 2013; Borowski et al., 2013; Jourdain et al., 2013; Lee et al., 2013). These RNA granules also contain RNA-binding proteins, methyltransferases, and ribosomal proteins, therefore likely representing the nucleoid-MIOREX complexes identified here. In addition to a role of the RNA granules in organizing the early steps of gene expression, it was demonstrated that also ribosome assembly occurs in proximity to the nucleoid (Bogenhagen et al., 2014; He et al., 2012). Because of technical difficulties in working with mitochondrial ribosomes, it was not known how the fully assembled ribosome is related to these structures. Surprisingly, our work provides evidence that ribosomes are tightly connected to RNA processing, maturation, and decay not only in RNA granules adjacent to the nucleoid but also in the form of the peripheral MIOREX complexes, thus establishing an expressosome-like assembly. Importantly, the exact relationship between the MIOREX complexes as revealed here and the RNA foci found in mammalian mitochondria can first be resolved when the technological advances from our study are applied to the studies of gene expression in the mammalian system. Nevertheless, a similar higher-order organization of protein synthesis was discovered in the mammalian cytoplasm, where kinetic experiments revealed that tRNA metabolism and the translation machinery are tightly linked (Stapulionis and Deutscher, 1995).

Whereas we have unraveled with this work the spatial organization of mitochondrial gene expression, our study also raises a number of fundamental questions on the sequences of events underlying protein synthesis in the organelle. One essential aspect of translation is initiation, where the mRNA is loaded onto the ribosome. Our data showing that many factors implicated in posttranscriptional mRNA metabolism interact specifically with the ribosome suggest that mitochondrial mRNAs do not freely diffuse in the matrix to find a translation-competent ribosome. Instead, mRNA maturation and translation apparently occur in a channeled fashion in the MIOREX complexes. Supportive evidence for such a model comes from the observation that mRNAs that were introduced into mitochondria by electroporation (McGregor et al., 2001) failed to be translated, although the transcripts stayed intact. Clearly, an obligatory channeled RNA metabolism would prevent those transcripts from entering the gene expression pathway spontaneously. Likewise, the reported interaction of Nam1 (that we identified in this work as a MIOREX constituent) with both the RNA polymerase and the translational activators points to a tight coupling between synthesis of the mRNA and its interaction with a specific translational activator at the inner membrane (Naithani et al., 2003; Rodeheffer et al., 2001; Rodeheffer and Shadel, 2003), supporting the idea that the newly transcribed mRNAs are channeled from transcription to translation.

Yeast mitochondrial RNA decay depends on the combined action of the helicase Suv3 and the RNase Dss1, forming the mitochondrial degradosome (Szczesny et al., 2012). Here, we revealed that Dss1 interacts specifically with the large ribosomal subunit, whereas Suv3 is mainly a component of the nucleoid-MIOREX complex, in line with previous observations that it copurifies with mitochondrial ribosomes (Dziembowski et al., 2003) and a cluster-like organization adjacent to RNA and DNA (Borowski et al., 2013). The interaction of an RNase with the ribosome is reminiscent of the situation in bacteria, where RNase R binding to the small ribosomal subunit (Malecki et al., 2014) both stabilizes the enzyme and sequesters it from undesired spontaneous nucleolytic activity (Liang and Deutscher, 2013). Only when the ribosome contains a damaged mRNA, RNase R is active to rescue the ribosome in a process known as transtranslation.

Rescue of mitochondrial ribosomes stalled on a damaged mRNA apparently works differently, because key components of the transtranslation process like transfer-messenger RNA are not present (Wesolowska et al., 2014). It is tempting to speculate that Dss1 supports a similar directed turnover of damaged mRNAs. Interestingly, we observed that Suv3 is a component of the nucleoid-MIOREX assembly and not part of the peripheral complexes, in line with previous data showing a preferential nucleoid interaction (Bogenhagen et al., 2014). Because Suv3 and Dss1 have to interact for efficient degradation (Malecki et al., 2007), this observation suggests a functional cycle of translation: MIOREX complexes adjacent to the nucleoid are charged with newly transcribed pre-mRNAs. These RNAs are then matured and translated on the peripheral MIOREX complexes, which likely supply mitochondrial translation products close to the sites where OXPHOS complexes are assembled. When the mRNA is damaged, the MIOREX complexes with the ribosome-bound Dss1 interact with the nucleoid-MIOREX-located helicase Suv3, thus reconstituting full-degradosome activity for removal of the mRNA. This prepares the MIOREX complexes for a new round of charging with pre-mRNA to resume the cycle. Importantly, this model is purely speculative and requires thorough testing. However, with the technical innovations and the inventory of MIOREX components as presented here, this and many other exciting aspects of mitochondrial gene expression can be addressed in the future.

EXPERIMENTAL PROCEDURES

Yeast Strains and Growth Media

Strains used in this study (Table S3) were isogenic to either the wild-type strain W303 or BY4741. ProteinAHis7- or GFP-tagged variants were generated by directed homologous recombination of a PCR product using a *HIS3* cassette for positive selection. *NUC1* was disrupted with a *URA3* cassette. Yeast cultures were grown in YP (1% yeast extract and 2% peptone) or minimal medium (0.17% yeast nitrogen base and 0.5% ammonium sulfate) supplemented with 2% dextrose, galactose, or glycerol.

~40 nm. Note that Atp4-GFP is largely homogenously distributed over the mitochondrial tubules, whereas Mrpl4-GFP and Rmd9-GFP are localized in clusters. A subfraction of the Mrpl4-GFP and Rmd9-GFP clusters was localized immediately adjacent to nucleoids (*) or colocalizing with them (**), although neither Mrpl4 nor Rmd9 were enriched at the nucleoids.

(D) Model of the organization of mitochondrial gene expression. The nucleoid-MIOREX complexes contain, besides the ribosome and the nucleoid, factors mediating ribosome assembly, translational activators, and RNA maturation and decay. The peripheral MIOREX complexes contain, with the exception of DNA metabolism enzymes, factors involved in mRNA maturation, translation, and decay. IMM, inner mitochondrial membrane; mt, mitochondrial.

Analysis and Purification of Mitochondrial Ribosomes

Mitochondria were lysed in 1% n-dodecyl β-D-maltoside, 10–300 mM KOAc, 5 mM MgOAc, 0.8 mM EDTA, 5 mM β- mercaptoethanol, 1 mM phenylmethanesulfonylfluoride, 1 mM spermidine, 1× complete protease inhibitor (Roche), 10 mM Tris/HCl (pH 7.4), and 5% glycerol at 4°C. The cleared lysate was either separated on a sucrose gradient (1–0.3 M sucrose in lysis buffer) or incubated for 60 min with GFP-Trap A beads (ChromoTek) at 4°C to purify GFP-tagged ribosomes. Bound complexes were eluted with tobacco etch virus protease and analyzed by mass spectrometry and/or western blotting.

Immunofluorescence Labeling and Dual-Color STED Superresolution Microscopy

Yeast cells expressing GFP-tagged proteins were grown in YPD medium to early exponential growth phase and fixed with formaldehyde. GFP-tagged proteins and mtDNA were decorated with antibodies against GFP or double-stranded DNA which were, in turn, detected by secondary antibodies labeled with Alexa Fluor 594 and KK114. STED images were recorded using a two-color STED 595 QUAD scanning microscope (Abberior Instruments). Besides smoothing with a 20 nm Gaussian and contrast stretching, no image processing was performed.

Miscellaneous Methods

Polyclonal antisera against Mhr1, Mrps5, and Pth4 were generated by injecting rabbits with recombinantly expressed and purified antigens. The antibody against protein A was obtained from Sigma. Isolation of mitochondria, northern blotting (Gruschke et al., 2011), step-gradient purification of isolated mitochondria (Meisinger et al., 2000), and quantitative mass spectrometry (Richter-Dennerlein et al., 2014) were performed as described.

SUPPLEMENTAL INFORMATION

Supplemental Information includes Supplemental Experimental Procedures, three figures, and three tables and can be found with this article online at http://dx.doi.org/10.1016/j.celrep.2015.01.012.

AUTHOR CONTRIBUTIONS

K.K., R.S., B.V.M.-H., C.A.W., and T. Lamkemeyer performed the experiments. All authors analyzed and discussed the data, and K.K., S.J., T. Langer, and M.O. wrote the manuscript. M.O. designed the study.

ACKNOWLEDGMENTS

We would like to thank all members of our groups as well as Carol Dieckmann (University of Arizona, USA), Tom Fox (Cornell University, USA), and the groups of Per Ljungdahl and Claes Andréasson (Stockholm University, Sweden) for stimulating discussions. Jodi Nunnari (University of California, USA), Toni Barrientos (University of Miami, USA), Alexander Tzagoloff (Columbia University, USA), and Pawel Golik (Warsaw University, Poland) are gratefully acknowledged for providing material. Work in our laboratory was supported by the Swedish research council (VR-NT), the Center for Biomembrane Research at Stockholm University, Carl Tryggers Foundation, and the Knut and Alice Wallenberg Foundation.

Received: August 21, 2014
Revised: November 17, 2014
Accepted: December 31, 2014
Published: February 12, 2015

REFERENCES

Amunts, A., Brown, A., Bai, X.C., Llácer, J.L., Hussain, T., Emsley, P., Long, F., Murshudov, G., Scheres, S.H., and Ramakrishnan, V. (2014). Structure of the yeast mitochondrial large ribosomal subunit. Science *343*, 1485–1489.

Antonicka, H., Sasarman, F., Nishimura, T., Paupe, V., and Shoubridge, E.A. (2013). The mitochondrial RNA-binding protein GRSF1 localizes to RNA granules and is required for posttranscriptional mitochondrial gene expression. Cell Metab. *17*, 386–398.

Bogenhagen, D.F., Martin, D.W., and Koller, A. (2014). Initial steps in RNA processing and ribosome assembly occur at mitochondrial DNA nucleoids. Cell Metab. *19*, 618–629.

Borowski, L.S., Dziembowski, A., Hejnowicz, M.S., Stepien, P.P., and Szczesny, R.J. (2013). Human mitochondrial RNA decay mediated by PNPase-hSuv3 complex takes place in distinct foci. Nucleic Acids Res. *41*, 1223–1240.

Chacinska, A., Rehling, P., Guiard, B., Frazier, A.E., Schulze-Specking, A., Pfanner, N., Voos, W., and Meisinger, C. (2003). Mitochondrial translocation contact sites: separation of dynamic and stabilizing elements in formation of a TOM-TIM-preprotein supercomplex. EMBO J. *22*, 5370–5381.

Costanzo, M.C., and Fox, T.D. (1990). Control of mitochondrial gene expression in *Saccharomyces cerevisiae*. Annu. Rev. Genet. *24*, 91–113.

Datta, K., Fuentes, J.L., and Maddock, J.R. (2005). The yeast GTPase Mtg2p is required for mitochondrial translation and partially suppresses an rRNA methyltransferase mutant, mrm2. Mol. Biol. Cell *16*, 954–963.

De Silva, D., Fontanesi, F., and Barrientos, A. (2013). The DEAD box protein Mrh4 functions in the assembly of the mitochondrial large ribosomal subunit. Cell Metab. *18*, 712–725.

Dziembowski, A., Piwowarski, J., Hoser, R., Minczuk, M., Dmochowska, A., Siep, M., van der Spek, H., Grivell, L., and Stepien, P.P. (2003). The yeast mitochondrial degradosome. Its composition, interplay between RNA helicase and RNase activities and the role in mitochondrial RNA metabolism. J. Biol. Chem. *278*, 1603–1611.

Fox, T.D. (2012). Mitochondrial protein synthesis, import, and assembly. Genetics *192*, 1203–1234.

Frazier, A.E., Taylor, R.D., Mick, D.U., Warscheid, B., Stoepel, N., Meyer, H.E., Ryan, M.T., Guiard, B., and Rehling, P. (2006). Mdm38 interacts with ribosomes and is a component of the mitochondrial protein export machinery. J. Cell Biol. *172*, 553–564.

Greber, B.J., Boehringer, D., Leitner, A., Bieri, P., Voigts-Hoffmann, F., Erzberger, J.P., Leibundgut, M., Aebersold, R., and Ban, N. (2014). Architecture of the large subunit of the mammalian mitochondrial ribosome. Nature *505*, 515–519.

Gruschke, S., Gröne, K., Heublein, M., Hölz, S., Israel, L., Imhof, A., Herrmann, J.M., and Ott, M. (2010). Proteins at the polypeptide tunnel exit of the yeast mitochondrial ribosome. J. Biol. Chem. *285*, 19022–19028.

Gruschke, S., Kehrein, K., Römpler, K., Gröne, K., Israel, L., Imhof, A., Herrmann, J.M., and Ott, M. (2011). Cbp3-Cbp6 interacts with the yeast mitochondrial ribosomal tunnel exit and promotes cytochrome *b* synthesis and assembly. J. Cell Biol. *193*, 1101–1114.

Gruschke, S., Römpler, K., Hildenbeutel, M., Kehrein, K., Kühl, I., Bonnefoy, N., and Ott, M. (2012). The Cbp3-Cbp6 complex coordinates cytochrome *b* synthesis with $bc(_1)$ complex assembly in yeast mitochondria. J. Cell Biol. *199*, 137–150.

Haffter, P., McMullin, T.W., and Fox, T.D. (1990). A genetic link between an mRNA-specific translational activator and the translation system in yeast mitochondria. Genetics *125*, 495–503.

Haffter, P., McMullin, T.W., and Fox, T.D. (1991). Functional interactions among two yeast mitochondrial ribosomal proteins and an mRNA-specific translational activator. Genetics *127*, 319–326.

Hällberg, B.M., and Larsson, N.G. (2014). Making proteins in the powerhouse. Cell Metab. *20*, 226–240.

Harner, M., Körner, C., Walther, D., Mokranjac, D., Kaesmacher, J., Welsch, U., Griffith, J., Mann, M., Reggiori, F., and Neupert, W. (2011). The mitochondrial contact site complex, a determinant of mitochondrial architecture. EMBO J. *30*, 4356–4370.

He, J., Cooper, H.M., Reyes, A., Di Re, M., Kazak, L., Wood, S.R., Mao, C.C., Fearnley, I.M., Walker, J.E., and Holt, I.J. (2012). Human C4orf14 interacts with the mitochondrial nucleoid and is involved in the biogenesis of the small mitochondrial ribosomal subunit. Nucleic Acids Res. *40*, 6097–6108.

Heublein, M., Burguillos, M.A., Vögtle, F.N., Teixeira, P.F., Imhof, A., Meisinger, C., and Ott, M. (2014). The novel component Kgd4 recruits the E3 subunit to the mitochondrial α-ketoglutarate dehydrogenase. Mol. Biol. Cell *25*, 3342–3349.

Hoppins, S., Collins, S.R., Cassidy-Stone, A., Hummel, E., Devay, R.M., Lackner, L.L., Westermann, B., Schuldiner, M., Weissman, J.S., and Nunnari, J. (2011). A mitochondrial-focused genetic interaction map reveals a scaffold-like complex required for inner membrane organization in mitochondria. J. Cell Biol. *195*, 323–340.

Jakobs, S., and Wurm, C.A. (2014). Super-resolution microscopy of mitochondria. Curr. Opin. Chem. Biol. *20*, 9–15.

Jia, L., Dienhart, M., Schramp, M., McCauley, M., Hell, K., and Stuart, R.A. (2003). Yeast Oxa1 interacts with mitochondrial ribosomes: the importance of the C-terminal region of Oxa1. EMBO J. *22*, 6438–6447.

Jourdain, A.A., Koppen, M., Wydro, M., Rodley, C.D., Lightowlers, R.N., Chrzanowska-Lightowlers, Z.M., and Martinou, J.C. (2013). GRSF1 regulates RNA processing in mitochondrial RNA granules. Cell Metab. *17*, 399–410.

Kehrein, K., Bonnefoy, N., and Ott, M. (2013). Mitochondrial protein synthesis: efficiency and accuracy. Antioxid. Redox Signal. *19*, 1928–1939.

Kornmann, B., and Walter, P. (2010). ERMES-mediated ER-mitochondria contacts: molecular hubs for the regulation of mitochondrial biology. J. Cell Sci. *123*, 1389–1393.

Lee, K.W., Okot-Kotber, C., LaComb, J.F., and Bogenhagen, D.F. (2013). Mitochondrial ribosomal RNA (rRNA) methyltransferase family members are positioned to modify nascent rRNA in foci near the mitochondrial DNA nucleoid. J. Biol. Chem. *288*, 31386–31399.

Liang, W., and Deutscher, M.P. (2013). Ribosomes regulate the stability and action of the exoribonuclease RNase R. J. Biol. Chem. *288*, 34791–34798.

Ling, F., and Shibata, T. (2002). Recombination-dependent mtDNA partitioning: in vivo role of Mhr1p to promote pairing of homologous DNA. EMBO J. *21*, 4730–4740.

Malecki, M., Jedrzejczak, R., Stepien, P.P., and Golik, P. (2007). *In vitro* reconstitution and characterization of the yeast mitochondrial degradosome complex unravels tight functional interdependence. J. Mol. Biol. *372*, 23–36.

Malecki, M., Bárria, C., and Arraiano, C.M. (2014). Characterization of the RNase R association with ribosomes. BMC Microbiol. *14*, 34.

McGregor, A., Temperley, R., Chrzanowska-Lightowlers, Z.M., and Lightowlers, R.N. (2001). Absence of expression from RNA internalised into electroporated mammalian mitochondria. Mol. Genet. Genomics *265*, 721–729.

Meisinger, C., Sommer, T., and Pfanner, N. (2000). Purification of *Saccharomcyes cerevisiae* mitochondria devoid of microsomal and cytosolic contaminations. Anal. Biochem. *287*, 339–342.

Mick, D.U., Fox, T.D., and Rehling, P. (2011). Inventory control: cytochrome *c* oxidase assembly regulates mitochondrial translation. Nat. Rev. Mol. Cell Biol. *12*, 14–20.

Naithani, S., Saracco, S.A., Butler, C.A., and Fox, T.D. (2003). Interactions among *COX1, COX2*, and *COX3* mRNA-specific translational activator proteins on the inner surface of the mitochondrial inner membrane of *Saccharomyces cerevisiae*. Mol. Biol. Cell *14*, 324–333.

Nouet, C., Bourens, M., Hlavacek, O., Marsy, S., Lemaire, C., and Dujardin, G. (2007). Rmd9p controls the processing/stability of mitochondrial mRNAs and its overexpression compensates for a partial deficiency of oxa1p in *Saccharomyces cerevisiae*. Genetics *175*, 1105–1115.

Richter, R., Rorbach, J., Pajak, A., Smith, P.M., Wessels, H.J., Huynen, M.A., Smeitink, J.A., Lightowlers, R.N., and Chrzanowska-Lightowlers, Z.M. (2010). A functional peptidyl-tRNA hydrolase, ICT1, has been recruited into the human mitochondrial ribosome. EMBO J. *29*, 1116–1125.

Richter-Dennerlein, R., Korwitz, A., Haag, M., Tatsuta, T., Dargazanli, S., Baker, M., Decker, T., Lamkemeyer, T., Rugarli, E.I., and Langer, T. (2014). DNAJC19, a mitochondrial cochaperone associated with cardiomyopathy, forms a complex with prohibitins to regulate cardiolipin remodeling. Cell Metab. *20*, 158–171.

Rodeheffer, M.S., and Shadel, G.S. (2003). Multiple interactions involving the amino-terminal domain of yeast mtRNA polymerase determine the efficiency of mitochondrial protein synthesis. J. Biol. Chem. *278*, 18695–18701.

Rodeheffer, M.S., Boone, B.E., Bryan, A.C., and Shadel, G.S. (2001). Nam1p, a protein involved in RNA processing and translation, is coupled to transcription through an interaction with yeast mitochondrial RNA polymerase. J. Biol. Chem. *276*, 8616–8622.

Schägger, H., and Pfeiffer, K. (2000). Supercomplexes in the respiratory chains of yeast and mammalian mitochondria. EMBO J. *19*, 1777–1783.

Sickmann, A., Reinders, J., Wagner, Y., Joppich, C., Zahedi, R., Meyer, H.E., Schönfisch, B., Perschil, I., Chacinska, A., Guiard, B., et al. (2003). The proteome of *Saccharomyces cerevisiae* mitochondria. Proc. Natl. Acad. Sci. USA *100*, 13207–13212.

Smits, P., Smeitink, J.A., van den Heuvel, L.P., Huynen, M.A., and Ettema, T.J. (2007). Reconstructing the evolution of the mitochondrial ribosomal proteome. Nucleic Acids Res. *35*, 4686–4703.

Stapulionis, R., and Deutscher, M.P. (1995). A channeled tRNA cycle during mammalian protein synthesis. Proc. Natl. Acad. Sci. USA *92*, 7158–7161.

Szczesny, R.J., Borowski, L.S., Malecki, M., Wojcik, M.A., Stepien, P.P., and Golik, P. (2012). RNA degradation in yeast and human mitochondria. Biochim. Biophys. Acta *1819*, 1027–1034.

Szyrach, G., Ott, M., Bonnefoy, N., Neupert, W., and Herrmann, J.M. (2003). Ribosome binding to the Oxa1 complex facilitates co-translational protein insertion in mitochondria. EMBO J. *22*, 6448–6457.

Vincent, R.D., Hofmann, T.J., and Zassenhaus, H.P. (1988). Sequence and expression of *NUC1*, the gene encoding the mitochondrial nuclease in *Saccharomyces cerevisiae*. Nucleic Acids Res. *16*, 3297–3312.

von der Malsburg, K., Müller, J.M., Bohnert, M., Oeljeklaus, S., Kwiatkowska, P., Becker, T., Loniewska-Lwowska, A., Wiese, S., Rao, S., Milenkovic, D., et al. (2011). Dual role of mitofilin in mitochondrial membrane organization and protein biogenesis. Dev. Cell *21*, 694–707.

Wesolowska, M.T., Richter-Dennerlein, R., Lightowlers, R.N., and Chrzanowska-Lightowlers, Z.M. (2014). Overcoming stalled translation in human mitochondria. Front. Microbiol. *5*, 374.

Williams, E.H., Butler, C.A., Bonnefoy, N., and Fox, T.D. (2007). Translation initiation in *Saccharomyces cerevisiae* mitochondria: functional interactions among mitochondrial ribosomal protein Rsm28p, initiation factor 2, methionyl-tRNA-formyltransferase and novel protein Rmd9p. Genetics *175*, 1117–1126.

Zeng, X., Barros, M.H., Shulman, T., and Tzagoloff, A. (2008). *ATP25*, a new nuclear gene of *Saccharomyces cerevisiae* required for expression and assembly of the Atp9p subunit of mitochondrial ATPase. Mol. Biol. Cell *19*, 1366–1377.

Cell Reports

Supplemental Information

Organization of Mitochondrial Gene Expression in Two Distinct Ribosome-Containing Assemblies

Kirsten Kehrein, Ramon Schilling, Braulio Vargas Möller-Hergt, Christian A. Wurm, Stefan Jakobs, Tobias Lamkemeyer, Thomas Langer, and Martin Ott

Extended experimental procedures

Separation of mitochondrial lysates on sucrose gradients

All steps were performed at 4 °C. 1 mg mitochondria were washed in SH buffer (10.000 x*g*, 10 min, 4°C) and lysed for 10 min in 285 µl lysis buffer (1% DDM, 10-300 mM KOAc, 5 mM MgOAc, 0.8 mM EDTA, 5 mM β- mercaptoethanol, 1 mM PMSF, 1 mM spermidine, 1x complete protease inhibitor (roche, Sweden), 10 mM Tris/HCl, pH 7.4, 5 % glycerol). After 10 min, the lysate was diluted 1:2 with dilution buffer (10-300 mM KOAc, 5 mM MgOAc, 0.8 mM EDTA, 5 mM β-mercaptoethanol, 1 mM PMSF, 1 mM spermidine, 10 mM Tris/HCl, pH 7.4, 5 % glycerol) and centrifuged for 5 min at 16.000 x*g*. Cleared lysate was then separated on a sucrose gradient (1 - 0.3 M sucrose, 0.1% DDM, 10-300 mM KOAc, 5 mM MgOAc, 0.8 mM EDTA, 5 mM β-mercaptoethanol, 1 mM PMSF, 1 mM spermidine, 10 mM Tris/HCl, pH 7.4) for 1 h at 370.000 x*g* in an SW60Ti rotor (Beckman Coulter, Fullerton, CA). Fractions were collected and proteins precipitated by addition of 12 % TCA.

Native purification of ribosomes and ribosome-associated complexes

Mitochondria from yeast strains expressing GFP-tagged Mrp1 or Mrpl4 were lysed for 10 min as above, cleared by centrifugation, and the lysate incubated for 60 min with GFP-Trap®_A beads (ChromoTek, Germany) at 4 °C. After incubation beads were allowed to sediment by gravity and washed four times with dilution buffer containing 0.1% DDM. Beads were resuspended in wash buffer with 50U TEV protease and incubated for 1 h at 4 °C and the eluted proteins analyzed by mass spectrometry and Western blotting.

Immunofluorescence labeling and dual color STED super- resolution microscopy:

Yeast cells expressing GFP tagged proteins were grown in YPD medium to early exponential growth phase ($OD_{600\ nm}$ = 0.45 - 0.7). After fixation with 3.7% formaldehyde in growth

medium (RT, 20 min), cells were harvested by centrifugation (800 x*g*, 3 min) and washed in PBS/sorbitol (137 mM NaCl, 3 mM KCl, 8 mM Na_2HPO_4, 1.5 mM KH_2PO_4, 10% (w/v) sorbitol, pH 7). Subsequently, the yeast cell wall was removed by zymolyase digestion (10 min, 30 °C). After washing in PBS/sorbitol, cells were attached to the surface of a poly-L-lysine coated cover slip. Following a blocking step (10 min, 2% (w/v) bovine serum albumine; 0.1% (v/v) Tween20/ SDS in PBS/ sorbitol), GFP tagged proteins and mtDNA were decorated using rabbit antibodies against GFP (abcam, Cambridge, UK) and a mouse antibody against dsDNA (Santa Cruz Biotechnology, Dallas, Tx, USA) (RT, 1h). The primary antibodies were decorated with secondary goat-anti-rabbit and sheep-anti-mouse antibodies (Jackson ImmunoResearch, West Grove, PA, USA) custom labelled with Alexa 594 and KK114. After several washing steps in blocking solution and sorbitol in PBS, the cells were mounted in mowiol containing DABCO.

STED images were recorded using a 2-color STED 595 QUAD scanning microscope (Abberior Instruments, Göttingen, Germany) in a frame sequential scanning scheme using 20 nm pixels, pixel dwell times of 40 µs, and a time gated detection (1.5 - 9.5 ns). Besides smoothing with a 20 nm Gaussian and contrast stretching no image processing was performed.

Figure S1, Mrp8 and Mrps2 are no structural companents of the ribosome. Related to figure 2.

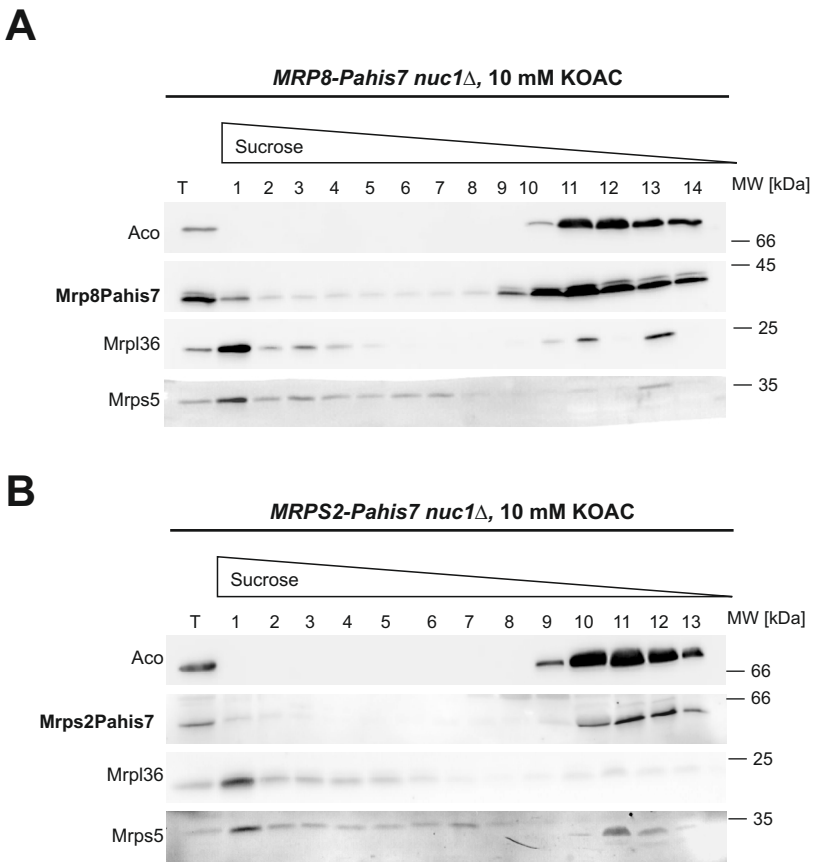

C

Name	Function	Ribosomal proteins part of the same regulon
Mrp8	Protein abundance increases in response to DNA replication stress	-
Mrps2	Protein with carboxyl methyl eserase activity	-
Ymr31	Subunit of alpha-ketoglutarate dehydrogenase	-

Figure S1: Mrp8, Mrps2 and Ymr31 are no structural components of the ribosome. Isolated mitochondria from the indicated strains were lysed for 10 min and the cleared lysates subjected to velocity centrifugation on a linear sucrose gradient. After separation of the lysate, fractions were collected starting from the bottom and analyzed by western blot. (A) Mrp8 does not co-migrate with the ribosome under low salt conditions. (B) Mrps2 does not co-migrate with the ribosome under low salt conditions. (C) Mrp8, Mrps2 and Ymr31 are not co-regulated with other ribosomal proteins. Co-regulation of Mrp8, Mrps2 and Ymr31 with ribosomal proteins was analyzed using SPELL (Hibbs et al. (2007)).

Figure S2. Interactions of mRNA metabolism factors with the ribosome. Related to figure 3.

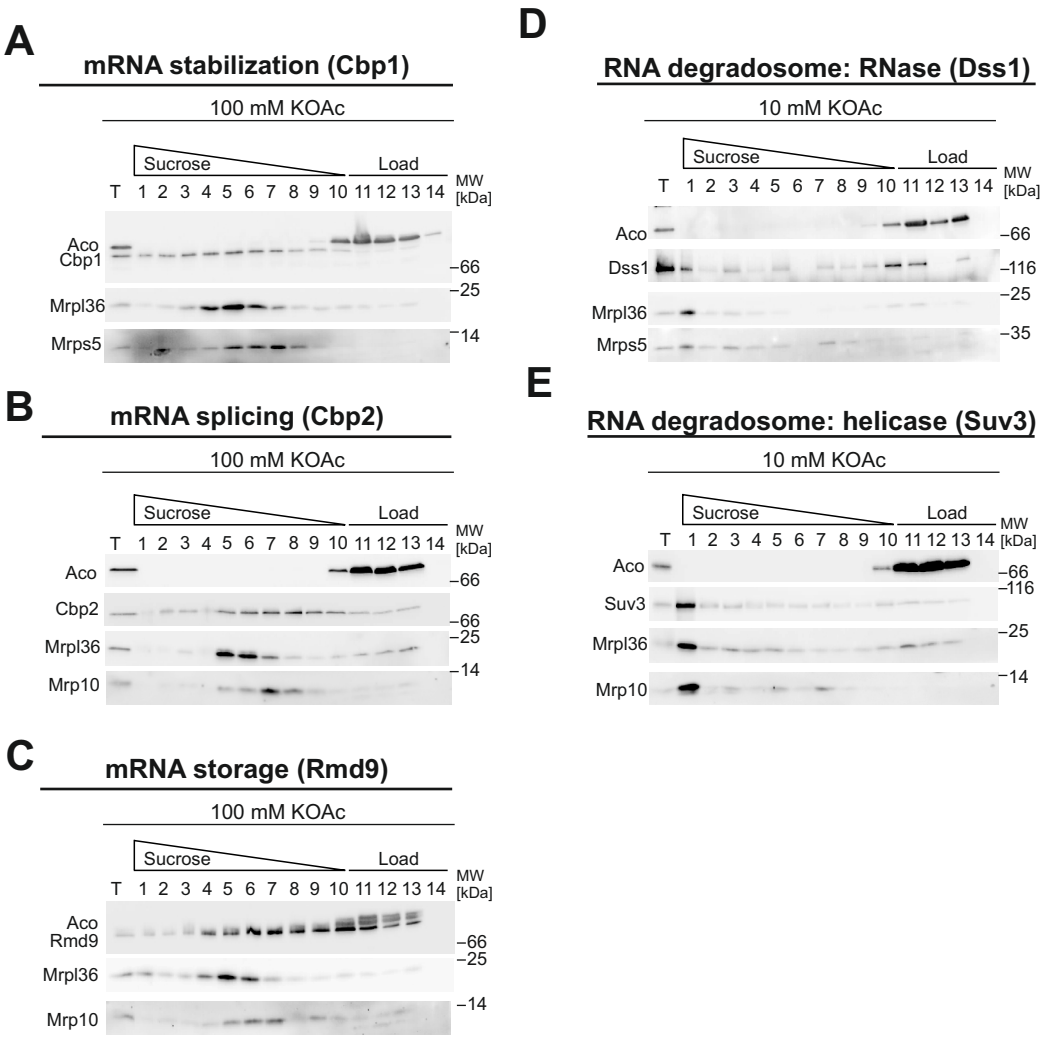

Figure S2: Interactions of selected factors supporting mRNA metabolism with mitochondrial ribosomes.
Isolated mitochondria from a strain expressing the indicated Prot.AHis7-tagged variant were lysed at the specified KOAc concentration for 10 min on ice and subjected to velocity centrifugation on a linear sucrose gradient. Fractions were analyzed by Western blotting.
T, total (representing 10% of the starting material); MW, molecular weight.

Figure S3, Mrpl4-GFP is part of both MIOREX complexes. Related to figure 5.

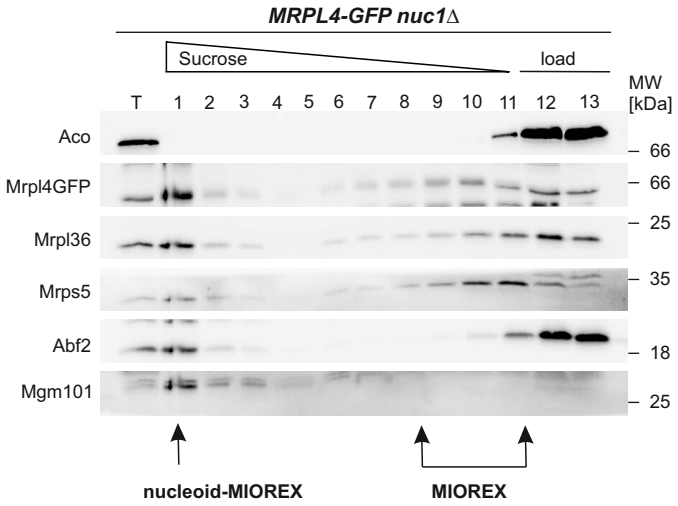

Figure S3: Mrpl4-GFP is part of the nucleoid-MIOREX and the peripheral MIOREX complexes.
Isolated mitochondria from a strain encoding a chromosomally GFP-tagged variant of Mrpl4 were lysed for 10 min on ice and subjected to velocity centrifugation on a linear sucrose gradient. Fractions were analyzed by Western blotting.
T, total (representing 10% of the starting material); MW, molecular weight.

Supplemental Table S1: Mass spectrometry of ribosomes purified under low salt conditions. Table S1 is found as a separate excel-sheet. Related to figure 2.

Supplemental Table S2: Mass spectrometry of ribosomes purified under high salt conditions. Table S2 is found as a separate excel-sheet. Related to figure 2.

Table S3, List of strains used in this study. Related to Experimental Procedures.

Name	Parental strain	Nuclear genotype	References
MOY663 W303Δnuc1 Cbs2Pahis7	W303	Mata; ura3-1; trp1Δ 2; leu2-3,112; his3-11,15; ade2-1; can1-100 CBS2Pahis7::HIS3 *nuc1*::URA3	This study
W303A		Mat a; ura3-1; trp1Δ 2; leu2-3,112; his3-11,15; ade2-1; can1-100	Thomas, B. J. & Rothstein, R. (1989)
MOY646 W303Δnuc1	W303	Mat a; ura3-1; trp1Δ 2; leu2-3,112; his3-11,15; ade2-1; can1-100 *nuc1*::URA3	This study
MOY 670 W303Δnuc1 Mrp1GFP	W303	Mat a; ura3-1; trp1Δ 2; leu2-3,112; his3-11,15; ade2-1; can1-100 MRP1GFP::TRP *nuc1*::URA3	This study
MOY942 W303Δnuc1 Rmd9GFP	W303	MATa; ura3-1; trp1Δ 2; leu2-3,112; his3-11,15; ade2-1; can1-100 RMD9GFP::HIS3 *nuc1*::URA3	This study
MOY653 W303Δnuc1 Mrpl4GFP	W303	Mat a; ura3-1; trp1Δ 2; leu2-3,112; his3-11,15; ade2-1; can1-100 MRPL4GFP::TRP *nuc1*::URA3	This study
MOY865 W303Δnuc1 Suv3Pahis7	W303	Mat a; ura3-1; trp1Δ 2; leu2-3,112; his3-11,15; ade2-1; can1-100 SUV3Pahis7::HIS3 *nuc1*::URA3	This study
MOY668 W303Δnuc1 Cbp1Pahis7	W303	Ma ta; ura3-1; trp1Δ 2; leu2-3,112; his3-11,15; ade2-1; can1-100 CBP1Pahis7::HIS3 *nuc1*::URA3	This study
MOY860 W303Δnuc1 Cbp2Pahis7	W303	Mat a; ura3-1; trp1Δ 2; leu2-3,112; his3-11,15; ade2-1; can1-100 CBP2Pahis7::HIS3 *nuc1*::URA3	This study
MOY859 W303Δnuc1 Rmd9Pahis7	W303	Mat a; ura3-1; trp1Δ 2; leu2-3,112; his3-11,15; ade2-1; can1-100 RMD9Pahis7::HIS3 *nuc1*::URA3	This study
MOY905 W303Δnuc1 Dss1Pahis7	W303	MATa; ura3-1; trp1Δ 2; leu2-3,112; his3-11,15; ade2-1; can1-100 DSS1Pahis7::HIS3 *nuc1*::URA3	This study
Atp4GFP	BY4741	MATa; his3Δ; leu2Δ0; met15Δ0; ura3Δ0; ATP4GFP::HIS3	Huh, WK et al Nature. (2003)